ACS EARTH AND SPACE CHEMISTRY

http://pubs.acs.org/journal/aesccq

Article

Kinetics Study of Acid-Catalyzed Sulfate Esterification Reactions for Atmospherically Relevant Polyols

Aziz C. L. Mohammed, Sunniva B. Sheffield, and Matthew J. Elrod*

Cite This: *ACS Earth Space Chem.* 2022, 6, 3115−3122

Read Online

ACCESS | Metrics & More | Article Recommendations

ABSTRACT: Extensive laboratory and field studies have identified organosulfates as important constituents of secondary organic aerosol (SOA). However, the mechanisms by which these organosulfates form in the atmosphere remain uncertain. The rate constants for the acid-catalyzed sulfate esterification reactions of a series of polyols were measured via bulk kinetics experiments using nuclear magnetic resonance (NMR) spectroscopy. The NMR data indicated that while reactions that occurred at a terminal hydroxyl site were somewhat faster than reactions at internal hydroxyl sites, there were no other significant structure−reactivity trends among the series of polyols. These results suggest that neighboring hydroxyl groups do not significantly modify the sulfate esterification rates from those previously determined for monoalcohols. Extrapolation of the kinetics data to typical atmospheric SOA acidities suggests that sulfate esterification reactions of polyols are unlikely to be a significant source of organosulfates. This conclusion is consistent with a previous study of monoalcohols which made similar conclusions about the kinetic infeasibility of this reaction type.

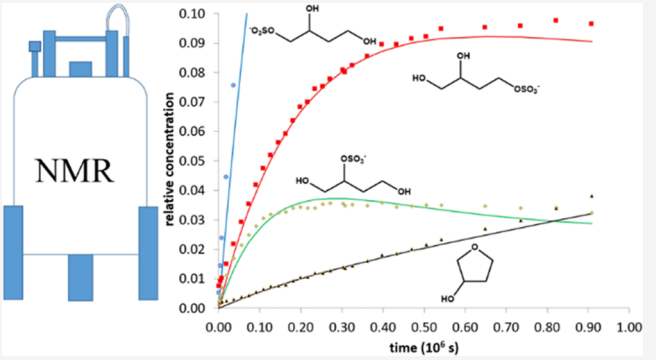

KEYWORDS: *atmosphere, air pollution, kinetics, organosulfate, sulfate esterification, nuclear magnetic resonance*

INTRODUCTION

Atmospheric aerosols have been implicated in human respiratory and cardiovascular disease[1] and affect global climate via scattering and absorption of radiation and the nucleation of clouds.[2] In particular, the atmospheric oxidation of volatile organic compounds (VOCs) plays a significant role in the production of secondary organic aerosol (SOA) formation, which is thought to make up the largest mass fraction of fine aerosol ($PM_{2.5}$, aerosol diameters of less than 2.5 μm).[3] The desire to identify human modifications to the aerosol content of the atmosphere has been of special interest in order to accurately model air quality and climate change. The synergistic interactions involving both biogenic and human-introduced VOCs with other compounds of anthropogenic origin are especially important to consider in this context. The observation of organosulfates ($R\text{-}OSO_3^-$) in atmospheric aerosols,[4] rain,[5] and clouds and fog[6,7] has been interpreted as key evidence for one such type of interaction. Specifically, the presence of organosulfates in the atmosphere originates from the condensed-phase reactions of VOC oxidation intermediates and inorganic sulfate, which itself is predominantly derived from the SO_2 emissions that often accompany fossil fuel utilization. The molecular formulas of dozens of organosulfates found in ambient atmospheric aerosols have now been identified by liquid chromatography−high-resolution mass spectrometry methods.[8−10]

There are a number of potential organosulfate-forming mechanisms in the atmosphere,[11] including ring-opening nucleophilic addition of sulfate to epoxides,[12−14] nucleophilic substitution of organonitrates by sulfate,[15,16] and sulfate radical addition to alkenes.[17−20] In the pioneering atmospheric chamber experiments by Surratt et al., because organosulfate formation was positively correlated with SOA acidity, it was suggested that organosulfates form by sulfate esterification of alcohols.[4] In this reaction, an alcohol group in the reactant is replaced by a sulfate group under strong acid catalysis conditions. The simultaneous observation of the isoprene-derived polyol species 2-methyltetrol (2-MT) and its sulfate derivative (2-MT-S)[4] lent credence to the potential viability of the sulfate esterification mechanism as a source of organosulfates in SOA. However, in a laboratory kinetics study of several model monoalcohols, it was shown that sulfate

Received: October 4, 2022
Revised: November 11, 2022
Accepted: November 16, 2022
Published: November 30, 2022

https://doi.org/10.1021/acsearthspacechem.2c00306
ACS Earth Space Chem. 2022, 6, 3115−3122

esterification reactions are likely too slow to proceed on atmospherically relevant timescales at typical SOA acidities.[21] Nevertheless, these experiments did not explore the potential effect of neighboring hydroxyl groups (which are common because of the ubiquity of polyols in the atmosphere) on the sulfate esterification rates. For example, neighboring hydroxyl groups in polyols could potentially accelerate sulfate esterification reaction rates via electronic interactions or could depress the rates via steric hindrance effects. Because the sulfate esterification mechanism is so general and can potentially explain the incorporation of a sulfate group into any alcohol precursor, it is important to definitively establish its kinetic feasibility for all alcohols (including polyols) in the atmosphere.

In the present study, we measure sulfate esterification rate constants in bulk aqueous sulfuric acid solutions using nuclear magnetic resonance (NMR) spectroscopy as the primary analytical technique. The bulk solution method allows for careful control over reactant and catalyst species, as well as their concentrations. The NMR method is used to determine isomer-specific structures and relative concentrations for product species. In contrast to the earlier study of simple monoalcohols,[21] the organosulfate-forming reactions of the polyols studied in the present work necessitate the use of a fully coupled kinetics method to extract the various rate constants. By systematically examining a series of polyols, structure−reactivity relationships (such as the role of neighboring hydroxyl groups) are determined. The extended-aerosol inorganics model (E-AIM)[22] and excess acidity[21,23−25] models are used to extrapolate the kinetics data to atmospherically relevant SOA acidities. Finally, the kinetic feasibility of sulfate esterification reactions for polyols under typical ambient SOA conditions is evaluated.

METHODS AND MATERIALS

Chemicals. The following reagents were acquired from the commercial sources Sigma Aldrich (sulfuric acid-d_2 solution 96−98 wt % in D_2O, 99.5 atom % D; methanol, 1-propanol, 99.9%; 1-butanol, anhydrous, 99.8%; ethylene glycol, 99.5%; 1,2-propanediol, 99.5%; 1,3-propanediol, 98%; glycerol, 99%; 1,2-butanediol, 98%; 1,3-butanediol, 99.5%; 1,4-butanediol, 99%; tetrahydrofuran, anhydrous, ≥99.9%, inhibitor free (THF); (±)-1,2,4-butanetriol, ≥90%; 3-hydroxytetrahydrofuran (THF-3-ol), 99%; meso-erythritol, 99%; 1,4-anhydroerythritol (THF-3,4-diol), 95%; and perchloric acid, 70%), Pharmco (methanol, glass purified, glass distilled HRGC/HPLC—Trace Grade; ethyl alcohol, 200 proof, absolute, anhydrous ACS/USP grade), and Cambridge Isotope Laboratories, Inc. (D_2O (D, 99.9%); sodium 2,2-dimethyl-2-silapentane-5-sulfonate (DSS)). 2-Methylbutane-1,2,3,4-tetrol (2-MT) was previously synthesized by our laboratory according to published procedures.[26]

Solution Preparation. Most solutions were prepared in deuterated solvents. All highly acidic solutions were prepared by slowly adding the appropriate ratio of deuterated acid, used as received, to D_2O in a 20 mL vial that was placed in a water bath to mitigate evaporation from the exothermic mixing process. Acidities for D_2SO_4/D_2O solutions were confirmed by measuring the mass of 1.00 mL of acid solution and comparing the density of the solution to a linear calibration curve relating density to mass fraction at room temperature, a relationship that was previously demonstrated for perchloric acid solutions.[27] The linear equation was derived from densities of titrated D_2SO_4/D_2O solutions and was found to be linear over the range from 45.1 to 72.5 wt %. Acidities were measured before each experiment to track any drift in the solution's weight percent resulting from variations in humidity. Reaction solutions were prepared by combining 10 μL of the alcohol of interest (10−15 mg in the case of solid reagents) with 1 mL of 55 wt % D_2SO_4, unless otherwise specified. Solutions were mixed for one minute, beginning at the time reagents were combined; this was recorded as $t = 0$ for the reaction. After mixing, approximately 750 μL of the solution was transferred to a 5 mm NMR tube, which was then capped and vortexed to ensure that the solution sat at the bottom of the tube. The use of concentrated 55 wt % D_2SO_4 solutions allowed for relatively fast data collection and significant production of organosulfates, which aided in the assembly and analysis of the NMR data.

NMR Methods. NMR experiments were conducted with a Bruker Avance Neo 400 MHz spectrometer using IconNMR and TopSpin software to schedule experiments and manage experimental parameters. All experiments were completed using built-in pulse sequences except when the sample was highly acidic or when the number of scans was increased to improve the signal-to-noise ratio. Experiments on highly acidic samples (e.g., 55 wt % D_2SO_4) were performed by turning off the automatic tuning and matching program and instead running the automatic tuning and matching program on a sample of 1 M D_2SO_4 in D_2O prior to every spectral acquisition. For experiments involving normal isotope 55 wt % H_2SO_4, the instrument was tuned as described above and shimmed and locked on a 55 wt % D_2SO_4 sample before running the 55 wt % H_2SO_4 sample.

NMR spectra were analyzed using Mnova Version 14 NMR software.[28] For ^{1}H experiments, the HDO solvent peak was referenced to 4.79 ppm, and for ^{13}C experiments, an internal standard of DSS was used where the methyl protons were referenced to 0.00 ppm.

Kinetics Methods. Kinetics monitoring was conducted using ^{1}H NMR whenever possible because fast ^{1}H nuclear spin relaxation leads to a linear relationship between the peak area and relative concentration. Between 10 and 20 spectra were collected until each system reached equilibrium, which was usually about 1 week for the reactions taking place in 55 wt % D_2SO_4. Therefore, the samples spent the vast majority of the time sitting in the autosampler queue and were only very occasionally inserted into the NMR for analysis. When ^{13}C NMR spectra were used to study kinetics, peaks for carbon nuclei with similar substitution environments were integrated to establish relative concentration ratios. This was necessary because carbon nuclei with different substitution environments have different ^{13}C relaxation times and lead to different amounts of detected signals during the standard 1 s relaxation time for ^{13}C experiments. Kinetics data were analyzed using the Mnova NMR reaction monitoring module in order to obtain raw integration values for the whole series of NMR spectra. The areas were adjusted to account for the number of hydrogen or carbon atoms per molecule represented in the peak and then normalized by dividing the adjusted peak area of one species by the sum of the adjusted peak areas for all species observed.

RESULTS AND DISCUSSION

NMR Assignments. Depending on the complexity of the reaction system, the ^{1}H NMR assignments could sometimes be

https://doi.org/10.1021/acsearthspacechem.2c00306
ACS Earth Space Chem. 2022, 6, 3115−3122

accomplished solely with the standard ^{1}H NMR spectra. However, the more complex reaction systems (such as triols and tetrols) often required ^{13}C, COSY, HSQC, and HMBC spectroscopies[29] to definitively establish the ^{1}H peak assignments that were necessary for the kinetics analysis. For example, the 1,3-propanediol system could be assigned solely from the ^{1}H spectrum. Figure 1 shows the equilibrium ^{1}H NMR spectrum of 1,3-propandiol reacting in 55 wt % D_2SO_4. Only two organosulfate products are possible (a single monosulfate and single disulfate), and they are both easily identified in the ^{1}H spectrum, even though there are some peak overlaps (A−A′ and C−C′) between the three species present at equilibrium. For 1,3-propanediol, time evolution of the concentrations of 1,3-propandiol, the monosulfate (MS1), and the disulfate (DS) could be straightforwardly tracked via the methylene protons (B, D, and E).

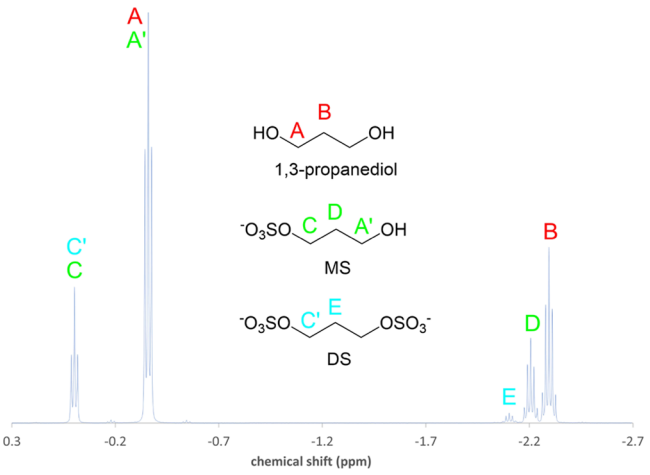

Figure 1. ^{1}H NMR spectrum for 1,3-propanediol in 55 wt % D_2SO_4 with peak assignments.

For systems in which many different mono- and disulfate species could form and for systems with 1,4-diol functionality which could form ring closure products, the ^{1}H spectra were much more difficult to assign. This complexity in species formation of the mono- and disulfate species was due to multiple hydroxyl groups and asymmetrical positioning of the hydroxyl groups. As shown in Figure 2, the equilibrium ^{1}H NMR spectrum of 1,2,4-butanetriol (1,2,4-BT) reacting in 55 wt % D_2SO_4 is an example of the potential complexities listed above. To assign the ^{1}H peaks for 1,2,4-BT, ^{1}H and ^{13}C NMR spectra of 1,2,4-BT in D_2O were first collected. The peak splittings observed suggested an atypical shift pattern where the D protons had a more positive chemical shift than the A protons. This was confirmed with the heteronuclear HSQC correlation experiment. After establishing the relative positions of all reactant peaks, the spectra from the 55 wt % D_2SO_4 kinetics experiment were analyzed. The t = 12.5 days spectrum was selected for peak assignment purposes because sufficient time had elapsed for the formation of significant amounts of products. ^{1}H, ^{13}C, COSY, HSQC, and HMBC correlation experiments were then conducted. Because the potential ring closure product (3-hydroxytetrahydrofuran, THF-3-ol) was commercially available, the sample was spiked with THF-3-ol and subjected to further ^{1}H and ^{13}C experiments to validate peak assignments. The spiking experiment definitively determined that peaks Q and R arose from THF-3-ol. The correlation experiments revealed that the E and J protons[21] arose from the MS1 and MS2 monosulfate isomers, respectively, while the MS2 and MS4 isomers overlapped at the position of the K and O peaks. The relative concentrations of the four product species were determined as follows: MS1 (E peak, 1 proton), MS2 (J peak, 1 proton), MS4 (K/O normalized to one proton, minus the contribution from MS2 as determined from the J peak), and THF-3-ol (Q peak, 1 proton). The relative concentration of the 1,2,4-BT reactant was determined by mass conservation (e.g., the relative concentrations must sum to unity) as follows: the total ^{1}H signal for all five species (1,2,4-BT and the four products) was determined by integrating over the chemical shift range from 1.1 to −3.1 ppm and dividing by 7 to normalize to a single proton. The 1,2,4-BT relative concentration was determined

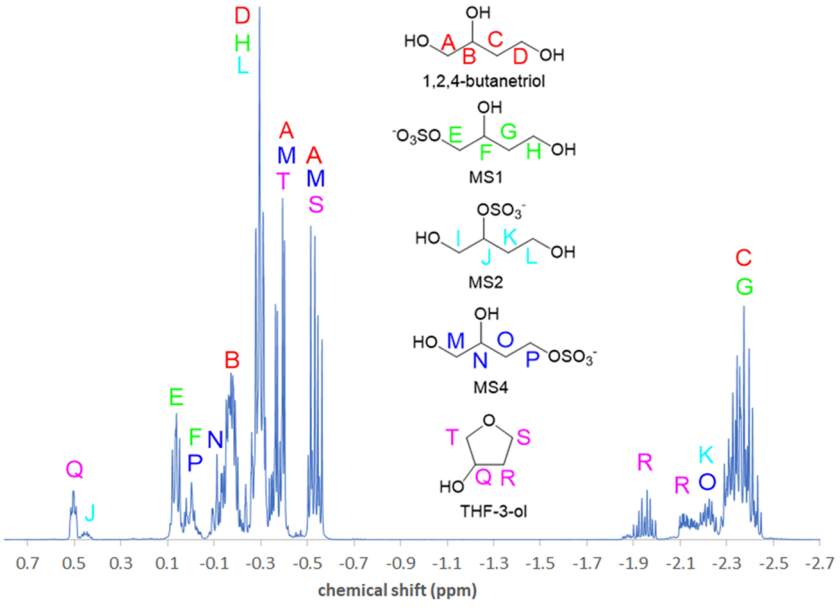

Figure 2. ^{1}H NMR spectrum on 1,2,4-butanetriol in 55 wt % D_2SO_4 with peak assignments.

https://doi.org/10.1021/acsearthspacechem.2c00306
ACS Earth Space Chem. 2022, 6, 3115−3122

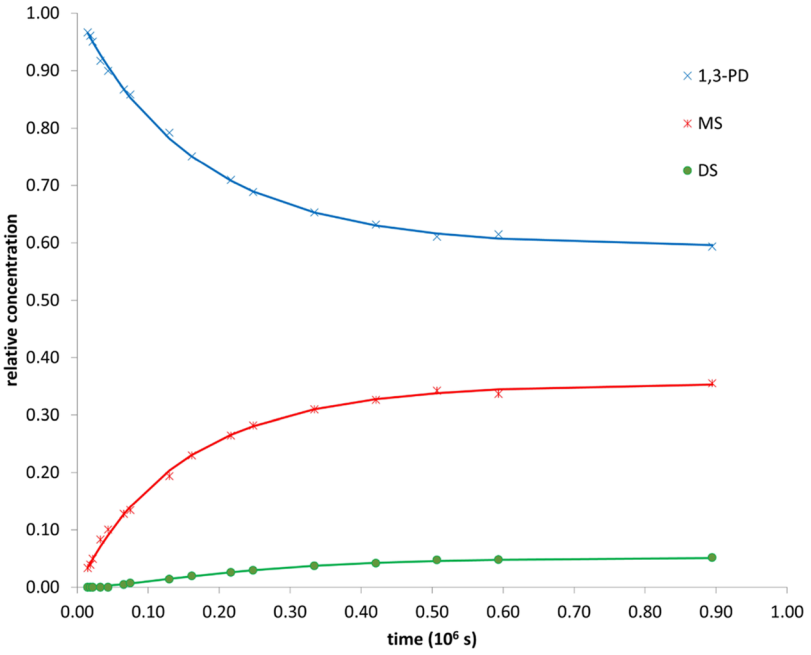

Figure 3. Plot of experimental data (symbols) and best-fitted lines for the three species present in the 1,3-propanediol 55 wt % D_2SO_4 system.

by subtracting the MS1, MS2, MS4, and THF-3-ol single proton relative concentrations from this total.

Kinetics Analysis. For systems in which the reactant and all major products could be individually quantified, the concentration vs time experimental data were fit to a minimal set of rate constants using the Kintecus modeling package.[30] In the case of the systems in which only organosulfate products formed, the reactant and product concentrations eventually reached equilibrium values. Because of the very slow ring-closure rates for the 1,4-diol species (e.g., τ = 165 days for 1,2,4-BT), it was not possible to monitor the solutions all the way to their equilibrium distribution point. However, previous computational thermodynamic studies indicated that similar THF-like cyclic species have free energies that are approximately 10 kcal/mol lower than their polyol precursors.[26] If this free energy difference is also typical of the systems studied in this work (such as that for 3-THF-ol and 1,2,4-BT), it is quite possible that 3-THF-ol would be the only species present at equilibrium.

Systems with Exclusive Organosulfate Products. The full mechanism for 1,3-propanediol, which is a representative system that forms only organosulfate products, is given below:

$$1,3-\mathrm{PD} + \mathrm{SO_4^{2-}} + \mathrm{H^+} \underset{\mathrm{H^+\,cat},k_{-\mathrm{MS1}}}{\overset{\mathrm{H^+\,cat},k_{\mathrm{MS1}}}{\rightleftharpoons}} \mathrm{MS1} + \mathrm{H_2O} \quad (1)$$

$$\mathrm{MS1} + \mathrm{SO_4^{2-}} + \mathrm{H^+} \underset{\mathrm{H^+\,cat},k_{-\mathrm{DS}}}{\overset{\mathrm{H^+\,cat},k_{\mathrm{DS}}}{\rightleftharpoons}} \mathrm{DS} + \mathrm{H_2O} \quad (2)$$

Because of the high concentrations of aqueous sulfuric acid solutions used, the concentrations of water, the proton reactant and catalyst, and the SO_4^{2-} nucleophile[31] were assumed to be constant relative to the alcohol reactants and organosulfate products. Therefore, the reaction mechanism could be represented by a series of reversible pseudo-first-order processes, shown below for 1,3-propandiol:

$$1,3-\mathrm{PD} \underset{\mathrm{H^+cat},k_{-\mathrm{MS1}}}{\overset{\mathrm{H^+\,cat},k_{\mathrm{MS1}}}{\rightleftharpoons}} \mathrm{MS1} \quad (3)$$

$$\mathrm{MS1} \underset{\mathrm{H^+\,cat},k_{-\mathrm{DS}}}{\overset{\mathrm{H^+\,cat},k_{\mathrm{DS}}}{\rightleftharpoons}} \mathrm{DS} \quad (4)$$

While the reaction mechanism of simple alcohols could be represented with a single reaction like that given in eq 3, the polyols, depending on the structure, could generate multiple singly sulfated species, doubly sulfated species, and for 1,4-polyols, ring closure products. In order to reduce the number of floating rate constant parameters in the Kintecus fits for the organosulfate product-only systems, the reverse rate constants were constrained by the equilibrium constant values. In particular, for 1,3-propanediol, the equilibrium constants K_3 and K_4 were easily determined from the ^{1}H NMR data, and the reverse rate constants $k_{-\mathrm{MS1}}$ and $k_{-\mathrm{DS}}$ could be constrained during the fitting of k_{MS1} and k_{DS} to the values of k_{MS1}/K_3 and k_{DS}/K_4, respectively, such that there were only two floating parameters in the Kintecus-driven fitting process, k_{MS1} and k_{DS}. More generally, based on the products formed for each polyol, the appropriate pseudo-first-order reactions were entered into a Kintecus Workbook, and the rate constants were fitted to experimental concentration vs time data. The results of this fitting process for 1,3-propanediol are shown in Figure 3. The forward and reverse isomer-specific monosulfate (MS) and disulfate (DS) rate constants (and the calculated equilibrium constants) for methanol, ethanol, ethylene glycol, 1-propanol, 1,2-propanediol, 1,3-propanediol, glycerol, 1-butanol, 1,2-butanediol, 1,3-butanediol, and 2,3-butanediol were determined in this fashion and are given in Tables 1 and 2.

Systems with Ring-Closure Product Formation. The existence of reaction systems with a thermodynamic product that dominated at long times, like reactants with 1,4-diol functionality, invalidated the use of the equilibrium constant constraint discussed above. This is because as time progressed, all organosulfate products were eventually converted back to polyols through the polyol-organosulfate equilibria reactions and then reacted to form the thermodynamically favored ring closure product. In this case, the forward and reverse rate constants had to be fitted independently. This procedure is

https://doi.org/10.1021/acsearthspacechem.2c00306
ACS Earth Space Chem. 2022, 6, 3115−3122

Table 1. MS1 and MS2 Rate and Equilibrium Constants in 55 wt% D_2SO_4[a]

	k_{MS1}	k_{-MS1}	K_1	k_{MS2}	k_{-MS2}	K_2
methanol	21	49	0.43			
ethanol	15	52	0.29			
ethylene glycol	16	100	0.16			
1-propanol	12	37	0.32			
1,2-propanediol	14	93	0.15	7.0	110	0.064
1,3-propanediol	25	41	0.61			
glycerol	66	87	0.76			
1-butanol	11	36	0.31			
1,2-butanediol	10	61	0.16	4.6	79	0.058
1,3-butanediol	16	94	0.17			
1,4-butanediol	43	45	0.96			
2,3-butanediol				6.2	86	0.072
1,2,4-butanetriol	25	33	0.76	6.3	100	0.063
meso-erythritol	20	61	0.33			

[a]Rate constants in 10^{-7} s^{-1} units.

explicitly described below for the 1,2,4-butanetriol system and Figure 4 gives the kinetics mechanism used in the analysis.

Figure 4 indicates that three kinetic products, MS1, MS2, and MS4, are formed via a reversible acid-catalyzed sulfate esterification process, while the fourth product, THF-3-ol, formed through an acid-catalyzed cyclodehydration mechanism. THF-3-ol was the most thermodynamically favorable product, and its formation was treated as irreversible. This mechanism was represented in the Kintecus software, and the experimental data was fit to the seven rate constants indicated above, with the results of the fit shown in Figure 5. The forward and reverse isomer-specific monosulfate (MS) formation rate constants (and the calculated equilibrium constants) and the forward THF formation rate constants for 1,4-butanediol, 1,2,4-butanetriol, and meso-erythritol were determined in this fashion and are given in Tables 1 and 2.

2-Methyltetrol System. The 2-methyltetrol (2-MT) reaction system was of particular interest because it could be a precursor of a number of previously identified organosulfates possessing the isoprene carbon backbone. Unfortunately, it was difficult to distinguish any organosulfate products from the reactant spectra due to spectral congestion arising from multiple diastereomeric isomer reactants and (presumably) multiple organosulfate products with structural and diastereomeric isomers. This was somewhat surprising as the tertiary center of 2-MT is capable of undergoing nucleophilic substitutions which should lead to a relatively easy-to-identify tertiary organosulfate species (because the methyl proton should be shifted higher than any other potential proton in the methyl chemical shift range and the tertiary carbon should be shifted higher than any other potential carbon nuclei).

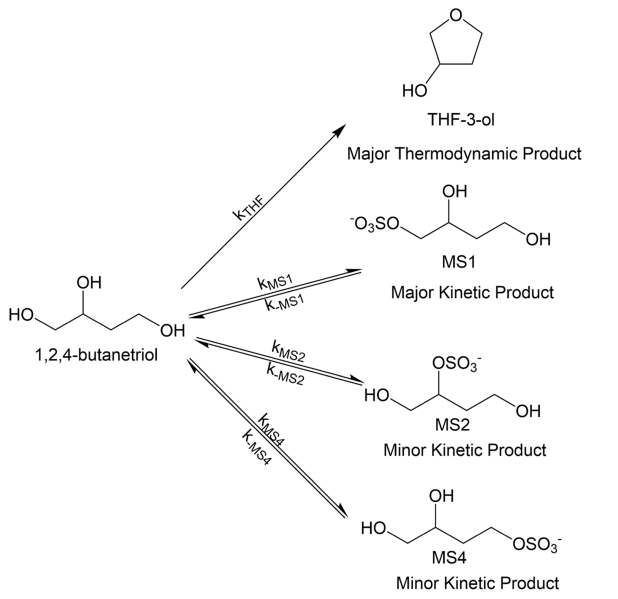

Figure 4. Assumed pseudo-first-order kinetics mechanism for the reaction of 1,2,4-butanetriol in 55 wt % D_2SO_4.

However, no evidence was obtained to confirm the formation of the tertiary organosulfate product. Previous kinetics studies of tertiary organosulfates showed that they can undergo much faster acid-catalyzed hydrolysis than primary or secondary organosulfates.[15] Therefore, it is possible that the tertiary organosulfate is a metastable species in 55 wt % D_2SO_4 that does not reach a steady-state concentration high enough to measure with the NMR method. The kinetics of the ring-closure mechanism for 2-MT was previously studied in the non-nucleophilic acid, 70 wt % $DClO_4$, and found to have a lifetime of about 0.1 day.[26] The excess acidity model[23] indicates that acid-catalyzed reactions in 55 wt % D_2SO_4 should occur about 3000 times more slowly than those in 70 wt % $DClO_4$. Therefore, the fact that the ring-closure product was not detected in the present 55 wt % D_2SO_4 experiments is consistent with the previously determined 70 wt % $DClO_4$ rate constants. In any case, no direct kinetics information could be extracted from the 2-MT system. However, because no special reactivity arising from the tertiary carbon center was detected, it is likely that the organosulfate-forming kinetics of 2-MT is similar to the kinetics of the S_N2-type sulfate esterification exhibited by the other polyols investigated in this work.

Uncertainties in Rate Constants. There were two primary sources of uncertainty in the rate constants: (1) the acidity of D_2SO_4 solutions prepared and (2) any errors that arose from the rate constant fitting process, which includes errors in the experimentally determined relative concentration data and the appropriateness of the assumed mechanism.

Table 2. MS3, MS4, DS, and THF Rate and Equilibrium Constants in 55 wt% D_2SO_4[a]

	k_{MS3} or k_{MS4}	k_{-MS3} or k_{-MS4}	K_3 or K_4	k_{DS}	k_{-DS}	K_{DS}	k_{THF}
ethylene glycol				25	350	0.071	
1,3-propanediol				14	98	0.14	
1,3-butanediol	3.3	24	0.14				
1,4-butanediol				12	140	0.086	5.1
1,2,4-butanetriol	7.0	38	0.18				0.70
meso-erythritol							1.5

[a]Rate constants in 10^{-7} s^{-1} units.

https://doi.org/10.1021/acsearthspacechem.2c00306
ACS Earth Space Chem. 2022, 6, 3115−3122

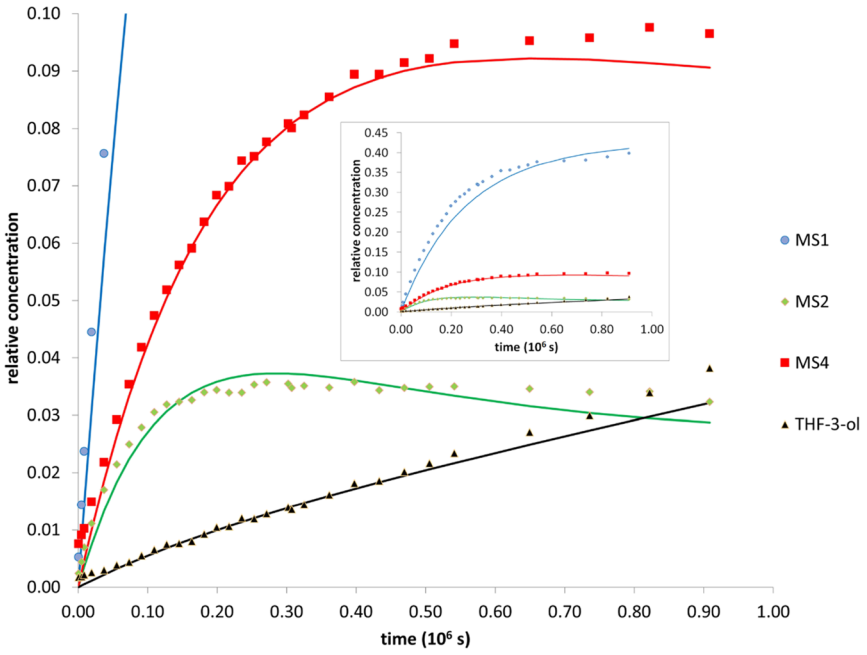

Figure 5. Plot of experimental data (symbols) and best fitted lines in the 1,2,4-butanetriol 55 wt % D_2SO_4 system. Inset plot: all four chemical species. Main plot: three lowest concentration chemical species.

Kintecus makes use of a proprietary algorithm to optimize the fit of the curve to experimental data, which makes the establishment of the uncertainties in the rate constants somewhat difficult. To address this issue, the "-CONF" switch was applied, which gave the confidence interval for the model and rate constant output. By varying the initial guess values to both extremes of the confidence interval for each parameter, it was possible to determine the approximate uncertainties associated with the rate constants. Combining the estimated uncertainties from Kintecus and acidity, it was determined that there was an uncertainty of about 25% in the rate constants for the more complicated analysis situations (such as the 1,2,4-butanetriol system) and substantially less for the simple situations (such as the 1,3-propanediol system). While the fitting process shows no obvious systematic error for the 1,3-propanediol system (as shown in Figure 3), there is some apparent systematic error for the 1,2,4-butanetriol system (as shown in Figure 5). While it is not possible to definitively identify the source of the systematic error, some possibilities include systematic errors in the quantitation from the NMR data and the occurrence of reactions other than those indicated in Figure 4.

Structure–Function Relationships. One of the main motivations of the systematic study of the sulfate esterification kinetics for a series of polyols, some of which are atmospherically abundant and some of which are not, was to discover structure–function relationships that could help predict the sulfate esterification kinetics of any atmospherically relevant polyol. The data in Tables 1 and 2 clearly indicate that for reactions at terminal hydroxyl positions, the forward rate and equilibrium constants are larger than those for internal hydroxyl positions, which is likely due to steric hindrance effects. Among the systems with reactions at the terminal hydroxyl position, there is some variation in the rate constants, but there is no obvious structural trend. For extrapolation purposes, the 55 wt % D_2SO_4 data indicate that a value of about 20×10^{-7} s^{-1} is an appropriate average value for the sulfate esterification rate constant at terminal hydroxyl positions and a value of about 5×10^{-7} s^{-1} is an appropriate average value for the sulfate esterification rate constant at internal hydroxyl positions. For the ring-closure kinetics, the data in Table 2 indicate that these reactions are generally similar to or slower than the internal hydroxyl position sulfate esterification reactions. For example, the ring-closure rate constant for 1,4-butanediol is similar to the rate constants for internal hydroxyl position sulfate esterification reactions, while the 1,2,4-butanetriol and meso-erythritol ring-closure reactions are slower. Steric hindrance effects are also the likely explanation for the slower ring-closure kinetics of the triol and tetrol systems.

Atmospheric Implications. In order to extrapolate the 55 wt % D_2SO_4 rate constants to more typical atmospheric conditions, both the higher pH and the normal isotope identity of acidic atmospheric aerosols must be considered. The previous study of the sulfate esterification reaction kinetics of monoalcohols[21] incorrectly used two different scales for pH to associate pH with H_2SO_4 weight percentage. This association is needed because the excess acidity model[23] is parametrized according to the weight percentage, whereas atmospheric aerosol acidity is usually reported as an effective pH value. The problem concerns the calculation of mole fraction-based proton activities in the E-AIM model[22] for a given H_2SO_4 weight percentage as opposed to the more common method of calculating pH from molality-based proton activities. This common inconsistency in aerosol pH reporting is discussed by Pye et al.[32] Estimates of ambient aerosol acidity indicate that the molality-based pH can sometimes reach values as low as pH = 0.[32] Using the correct pH-wt % association, the E-AIM model predicts that a molality-based pH of zero corresponds to about 10 wt % H_2SO_4. The excess acidity model[23] indicates that the rate of acid-catalyzed reactions at 10 wt % H_2SO_4 should be slower than reactions at 55 wt % H_2SO_4 by a factor of about 340. The isotope effect on the rate constants was directly measured by comparing the rate constants for

https://doi.org/10.1021/acsearthspacechem.2c00306
ACS Earth Space Chem. 2022, 6, 3115−3122

methanol reacting in both 55 wt % D_2SO_4 and H_2SO_4. The experiments indicated that the sulfate esterification rate slowed by a factor of 3 in normal isotope sulfuric acid as compared to deuterated sulfuric acid, which is quantitatively consistent with the inverse isotope effect often associated with acid-catalyzed mechanisms.[33] Therefore, to extrapolate the present 55 wt % D_2SO_4 rate constants to ambient atmospheric aerosols with an effective pH of zero and normal isotope sulfuric acid content, the rate constant values should be divided by a factor of about 1000. Table 3 contains the predicted pH = 0 atmospheric aerosol lifetimes ($\tau = 1/k$) for sulfate esterification reactions occurring at the (faster) terminal hydroxyl position for an atmospherically relevant representative mono, di, tri, and tetra-ol species. It is clear that the presence of multiple hydroxyl groups in polyols do not substantially change the sulfate esterification rate constants from the values of the rate constants of the monoalcohols previously measured by Minerath et al.[21] Therefore, it is a relatively simple matter to estimate sulfate esterification lifetimes for any potential atmospherically relevant polyol species. It should be noted that these extrapolated lifetimes are significantly longer than those estimated by Minerath et al. mainly due to the pH-wt % association discrepancy discussed earlier. Of course, because the ring-closure products were found to form even more slowly than the organosulfates, it is also expected that they will not form from these reactions on typical atmospheric time scales, even though they may be the favored thermodynamic product.

Table 3. Extrapolated Terminal Sulfate Esterification Lifetimes for pH = 0 (10 wt %) H_2SO_4

	pH = 0 lifetime (year)
methanol	15
ethylene glycol	20
glycerol	4.9
meso-erythritol	16

Of course, because these lifetimes are for bulk proxy solutions, the microenvironment on an actual aerosol particle could lead to reaction rates different from these values. However, in a review of rate acceleration phenomena in microdroplets, Wei et al. reported that no such accelerations have yet been observed for the S_N2 reaction mechanism,[34] the presumed mechanism type for sulfate esterification reactions. Because atmospheric aerosol lifetimes are predicted to be on the order of 1−2 weeks (0.02−0.04 years),[35,36] it is clear that the sulfate esterification reactions are predicted to be a factor of about 100−1000 times too slow to be atmospherically relevant. Therefore, any aerosol environment-specific rate acceleration would have to be very significant for these reactions to be kinetically competitive. In conclusion, sulfate esterification reactions are unlikely to be kinetically feasible mechanisms for the formation of organosulfates from atmospheric polyol species.

AUTHOR INFORMATION

Corresponding Author

Matthew J. Elrod − *Department of Chemistry and Biochemistry, Oberlin College, Oberlin, Ohio 44074, United States;* orcid.org/0000-0002-1656-8261; Email: mjelrod@oberlin.edu

Authors

Aziz C. L. Mohammed − *Department of Chemistry and Biochemistry, Oberlin College, Oberlin, Ohio 44074, United States*

Sunniva B. Sheffield − *Department of Chemistry and Biochemistry, Oberlin College, Oberlin, Ohio 44074, United States*

Complete contact information is available at: https://pubs.acs.org/10.1021/acsearthspacechem.2c00306

Notes

The authors declare no competing financial interest.

ACKNOWLEDGMENTS

We thank Santino Stropoli for providing the 2-MT sample and Adriana Morales for her assistance in the collection of the kinetics data. This material is based upon work supported by the National Science Foundation under Grant No. 1841019.

REFERENCES

(1) West, J. J.; Cohen, A.; Dentener, F.; Brunekreef, B.; Zhu, T.; Armstrong, B.; Bell, M. L.; Brauer, M.; Carmichael, G.; Costa, D. L.; Dockery, D. W.; Kleeman, M.; Krzyzanowski, M.; Kunzli, N.; Liousse, C.; Lung, S. C.; Martin, R. V.; Poschl, U.; Pope, C. A., 3rd; Roberts, J. M.; Russell, A. G.; Wiedinmyer, C. What We Breathe Impacts Our Health: Improving Understanding of the Link between Air Pollution and Health. *Environ. Sci. Technol.* **2016**, *50*, 4895−4904.

(2) Kroll, J. H.; Seinfeld, J. H. Chemistry of Secondary Organic Aerosol: Formation and Evolution of Low-Volatility Organics in the Atmosphere. *Atmos. Environ.* **2008**, *42*, 3593−3624.

(3) Hallquist, M.; Wenger, J. C.; Baltensperger, U.; Rudich, Y.; Simpson, D.; Claeys, M.; Dommen, J.; Donahue, N. M.; George, C.; Goldstein, A. H.; Hamilton, J. F.; Herrmann, H.; Hoffmann, T.; Iinuma, Y.; Jang, M.; Jenkin, M. E.; Jimenez, J. L.; Kiendler-Scharr, A.; Maenhaut, W.; McFiggans, G.; Mentel, T. F.; Monod, A.; Prevot, A. S. H.; Seinfeld, J. H.; Surratt, J. D.; Szmigielski, R.; Wildt, J. The Formation, Properties and Impact of Secondary Organic Aerosol: Current and Emerging Issues. *Atmos. Chem. Phys.* **2009**, *9*, 5155−5236.

(4) Surratt, J. D.; Kroll, J. H.; Kleindienst, T. E.; Edney, E. O.; Claeys, M.; Sorooshian, A.; Ng, N. L.; Offenberg, J. H.; Lewandowski, M.; Jaoui, M.; Flagan, R. C.; Seinfeld, J. H. Evidence for Organosulfates in Secondary Organic Aerosol. *Environ. Sci. Technol.* **2007**, *41*, 517−527.

(5) Altieri, K. E.; Turpin, B. J.; Seitzinger, S. P. Oligomers, Organosulfates, and Nitrooxy Organosulfates in Rainwater Identified by Ultra-High Resolution Electrospray Ionization Ft-Icr Mass Spectrometry. *Atmos. Chem. Phys.* **2009**, *9*, 2533−2542.

(6) Boone, E. J.; Laskin, A.; Laskin, J.; Wirth, C.; Shepson, P. B.; Stirm, B. H.; Pratt, K. A. Aqueous Processing of Atmospheric Organic Particles in Cloud Water Collected Via Aircraft Sampling. *Environ. Sci. Technol.* **2015**, *49*, 8523−8530.

(7) Pratt, K. A.; Fiddler, M. N.; Shepson, P. B.; Carlton, A. G.; Surratt, J. D. Organosulfates in Cloud Water above the Ozarks' Isoprene Source Region. *Atmos. Environ.* **2013**, *77*, 231−238.

(8) Cai, D.; Wang, X.; Chen, J.; Li, X. Molecular Characterization of Organosulfates in Highly Polluted Atmosphere Using Ultra-High-Resolution Mass Spectrometry. *J. Geophys. Res.: Atmos.* **2020**, *125*, No. e2019JD032253.

(9) Hughes, D. D.; Christiansen, M. B.; Milani, A.; Vermeuel, M. P.; Novak, G. A.; Alwe, H. D.; Dickens, A. F.; Pierce, R. B.; Millet, D. B.; Bertram, T. H.; Stanier, C. O.; Stone, E. A. Pm2.5 Chemistry, Organosulfates, and Secondary Organic Aerosol During the 2017 Lake Michigan Ozone Study. *Atmos. Environ.* **2021**, No. 117939.

(10) Wang, Y.; Ma, Y.; Li, X.; Kuang, B. Y.; Huang, C.; Tong, R.; Yu, J. Z. Monoterpene and Sesquiterpene Alpha-Hydroxy Organosulfates:

Synthesis, MS/MS Characteristics, and Ambient Presence. *Environ. Sci. Technol.* **2019**, *53*, 12278−12290.
(11) Bruggemann, M.; Xu, R.; Tilgner, A.; Kwong, K. C.; Mutzel, A.; Poon, H. Y.; Otto, T.; Schaefer, T.; Poulain, L.; Chan, M. N.; Herrmann, H. Organosulfates in Ambient Aerosol: State of Knowledge and Future Research Directions on Formation, Abundance, Fate, and Importance. *Environ. Sci. Technol.* **2020**, *54*, 3767−3782.
(12) Minerath, E. C.; Elrod, M. J. Assessing the Potential for Diol and Hydroxy Sulfate Ester Formation from the Reaction of Epoxides in Tropospheric Aerosols. *Environ. Sci. Technol.* **2009**, *43*, 1386−1392.
(13) Surratt, J. D.; Chan, A. W. H.; Eddingsaas, N. C.; Chan, M.; Loza, C. L.; Kwan, A. J.; Hersey, S. P.; Flagan, R. C.; Wennberg, P. O.; Seinfeld, J. H. Reactive Intermediates Revealed in Secondary Organic Aerosol Formation from Isoprene. *Proc. Natl. Acad. Sci. U. S. A.* **2010**, *107*, 6640−6645.
(14) Eddingsaas, N. C.; VanderVelde, D. G.; Wennberg, P. O. Kinetics and Products of the Acid-Catalyzed Ring-Opening of Atmospherically Relevant Butyl Epoxy Alcohols. *J. Phys. Chem. A* **2010**, *114*, 8106−8113.
(15) Hu, K. S.; Darer, A. I.; Elrod, M. J. Thermodynamics and Kinetics of the Hydrolysis of Atmospherically Relevant Organonitrates and Organosulfates. *Atmos. Chem. Phys.* **2011**, *11*, 8307−8320.
(16) Darer, A. I.; Cole-Filipiak, N. C.; O'Connor, A. E.; Elrod, M. J. Formation and Stability of Atmospherically Relevant Isoprene-Derived Organosulfates and Organonitrates. *Environ. Sci. Technol.* **2011**, *45*, 1895−1902.
(17) Schone, L.; Schindelka, J.; Szeremeta, E.; Schaefer, T.; Hoffmann, D.; Rudzinski, K. J.; Szmigielski, R.; Herrmann, H. Atmospheric Aqueous Phase Radical Chemistry of the Isoprene Oxidation Products Methacrolein, Methyl Vinyl Ketone, Methacrylic Acid and Acrylic Acid–Kinetics and Product Studies. *Phys. Chem. Chem. Phys.* **2014**, *16*, 6257−6272.
(18) Schindelka, J.; Iinuma, Y.; Hoffmann, D.; Herrmann, H. Sulfate Radical-Initiated Formation of Isoprene-Derived Organosulfates in Atmospheric Aerosols. *Faraday Discuss.* **2013**, *165*, 237.
(19) Ren, H.; Sedlak, J. A.; Elrod, M. J. General Mechanism for Sulfate Radical Addition to Olefinic Volatile Organic Compounds in Secondary Organic Aerosol. *Environ. Sci. Technol.* **2021**, *55*, 1456−1465.
(20) Cope, J. D.; Bates, K. H.; Tran, L. N.; Abellar, K. A.; Nguyen, T. B. Sulfur Radical Formation from the Tropospheric Irradiation of Aqueous Sulfate Aerosols. *Proc. Natl. Acad. Sci. U. S. A.* **2022**, *119*, No. e2202857119.
(21) Minerath, E. C.; Casale, M. T.; Elrod, M. J. Kinetics Feasibility Study of Alcohol Sulfate Esterification Reactions in Tropospheric Aerosols. *Environ. Sci. Technol.* **2008**, *42*, 4410−4415.
(22) Wexler, A. S.; Clegg, S. L. Atmospheric Aerosol Models for Systems Including the Ions H^+, NH_4^+, Na^+, SO_4^{2-}, NO_3^-, Cl^-, Br^-, and H_2O. *J. Geophys. Res.* **2002**, *107*, No. JD000451.
(23) Cox, R. A.; Yates, K.; Acidities, E. A Generalized Method for the Determination of Basicities in Aqueous Acid Mixtures. *J. Am. Chem. Soc.* **1978**, *100*, 3861−3867.
(24) Baigrie, L. M.; Cox, R. A.; Slebocka-Tilk, H.; Tencer, M.; Tidwell, T. T. Acid-Catalyzed Enolization and Aldol Condensation of Acetaldehyde. *J. Am. Chem. Soc.* **1985**, *107*, 3640−3645.
(25) Casale, M.; Richman, A.; Elrod, M.; Garland, R.; Beaver, M.; Tolbert, M. Kinetics of Acid-Catalyzed Aldol Condensation Reactions of Aliphatic Aldehydes. *Atmos. Environ.* **2007**, *41*, 6212−6224.
(26) Watanabe, A. C.; Stropoli, S. J.; Elrod, M. J. Assessing the Potential Mechanisms of Isomerization Reactions of Isoprene Epoxydiols on Secondary Organic Aerosol. *Environ. Sci. Technol.* **2018**, *52*, 8346−8354.
(27) Brickwedde, L. H. Properties of Aqueous Solutions of Perchloric Acid. *J. Res. Nat. Bur. Stand. (U.S.)* **1949**, *42*, 309.
(28) Willcott, M. R. Mestre Nova. *J. Am. Chem. Soc.* **2009**, *131*, 13180−13180.
(29) Braun, S.; Kalinowski, H.-O.; Berger, S.*150 and More Basic Nmr Experiments*; Wiley-VCH: Weinheim, 1998.
(30) Ianni, J.*Kintecus*, V3.95, www.kintecus.com.
(31) Aoki, E.; Sarrimanolis, J. N.; Lyon, S. A.; Elrod, M. J. Determining the Relative Reactivity of Sulfate, Bisulfate, and Organosulfates with Epoxides on Secondary Organic Aerosol. *ACS Earth Space Chem.* **2020**, *4*, 1793−1801.
(32) Pye, H. O. T.; Nenes, A.; Alexander, B.; Ault, A. P.; Barth, M. C.; Clegg, S. L.; Collett, J. L., Jr.; Fahey, K. M.; Hennigan, C. J.; Herrmann, H.; Kanakidou, M.; Kelly, J. T.; Ku, I. T.; McNeill, V. F.; Riemer, N.; Schaefer, T.; Shi, G.; Tilgner, A.; Walker, J. T.; Wang, T.; Weber, R.; Xing, J.; Zaveri, R. A.; Zuend, A. The Acidity of Atmospheric Particles and Clouds. *Atmos. Chem. Phys.* **2020**, *20*, 4809−4888.
(33) Laidler, K. J.*Chemical Kinetics*, 3rd edition; Harper & Row: New York, 1987.
(34) Wei, Z.; Li, Y.; Cooks, R. G.; Yan, X. Accelerated Reaction Kinetics in Microdroplets: Overview and Recent Developments. *Annu. Rev. Phys. Chem.* **2020**, *71*, 31−51.
(35) Hodzic, A.; Kasibhatla, P. S.; Jo, D. S.; Cappa, C. D.; Jimenez, J. L.; Madronich, S.; Park, R. J. Rethinking the Global Secondary Organic Aerosol (SOA) Budget: Stronger Production, Faster Removal, Shorter Lifetime. *Atmos. Chem. Phys.* **2016**, *16*, 7917−7941.
(36) Kristiansen, N. I.; Stohl, A.; Olivié, D. J. L.; Croft, B.; Søvde, O. A.; Klein, H.; Christoudias, T.; Kunkel, D.; Leadbetter, S. J.; Lee, Y. H.; Zhang, K.; Tsigaridis, K.; Bergman, T.; Evangeliou, N.; Wang, H.; Ma, P. L.; Easter, R. C.; Rasch, P. J.; Liu, X.; Pitari, G.; Di Genova, G.; Zhao, S. Y.; Balkanski, Y.; Bauer, S. E.; Faluvegi, G. S.; Kokkola, H.; Martin, R. V.; Pierce, J. R.; Schulz, M.; Shindell, D.; Tost, H.; Zhang, H. Evaluation of Observed and Modelled Aerosol Lifetimes Using Radioactive Tracers of Opportunity and an Ensemble of 19 Global Models. *Atmos. Chem. Phys.* **2016**, *16*, 3525−3561.

https://doi.org/10.1021/acsearthspacechem.2c00306
ACS Earth Space Chem. 2022, 6, 3115−3122